



TECHNICAL UNIVERSITY OF CLUJ-NAPOCA

ACTA TECHNICA NAPOCENSIS

Series: Applied Mathematics, Mechanics, and Engineering

Vol. 68, Issue II, June, 2025

RESISTIVE-LASER HYBRID SOURCE FOR FFF PRINTING PROCESS

Remus SOCOL, Iulian ȘTEFAN, Traian ȚUNESCU, Cristian CHIHAIA,
Nicușor-Alin SÎRBU, Ionel-Dănuț SAVU

Abstract: Some authors have reported the use of hybrid sources for heating the materials to be processed in various joining or sintering situations. The paper presents exploratory research on the use of a hybrid heating source, consisting of a resistive extrusion head and a defocused laser beam, to heat the material deposited in 3D printing by the FFF process. This hybrid source aims to reduce the cooling rate of the deposited material to improve the joining between two successive layers. It was also aimed at improving the degree of filling through an estimated flattening of the deposited filament. A simulation of the action of the hybrid heating source was carried out to determine the process parameters. A thermally stressed geometric model similar to the real situation was made. The thermal fields were simulated for different positions of the hybrid source on the part surface. When the temperatures estimated to achieve the proposed ones were reached, the thermal system data were taken and transferred to the physical 3D printing system. Deposits were made with these parameters, measuring the temperature values at various points of the thermal field on the surface of the part. The measurements confirmed the geometric model required by the simulation of the real thermal field. The samples made were visually analyzed and it was concluded that the deposit no longer has a circular section, but has flattened, which confirms the initial estimates: the degree of filling has increased by $x\%$.

Keywords: FFF printing, hybrid thermal source, defocused laser, modelling and simulation, thermal field measurement, visual testing.

1. INTRODUCTION

One of the 3D printing processes, in terms of application volume (from the household area to the top industry) is the Fused Filament Fabrication (FFF) process [1], [2], [3]. The development of products through this manufacturing process has become particularly accessible in the last 15 years [4], [5], [6]. There are a large number of 3D printer manufacturers for this process [7], there are a large number of types and families of 3D printers [8], [9], their costs have dropped to around €300 for a printer that can make parts with the volume of 100 x 100 x 100 mm, and the price of consumables has also dropped a lot [10]. For this reason, at least for rapid prototyping, the FFF 3D printing process is more than recommended. Studies published by various authors [11], [12], [13], [14], highlight the fact that for 3D printing by the FFF process the preferred consumables are polylactic acid (PLA), acrylonitrile - butadiene - styrene

(ABS), polyethylene terephthalate glycol (PETG), thermoplastic polyurethane (TPU), polyamide (Nylon), and the polycarbonate (PC).

The rapid development of this process was mainly due to the fact that patented elements became publicly accessible achievements. After this moment, research began to optimize the submission process. Northcutt et al. [15] analyzed how the level of crystalline organization of the material influences the characteristics of the deposited material. They found that the crystalline material is more fluid at the printing temperature, a situation that could favor the behavior of the deposited material heated with a hybrid source. These researchers also found that the polymer in a fluid-viscous state when transferred through the extrusion nozzle undergoes extremely fast shearing phenomena. Similarly, Liao [16] reports an improvement in the plasticity and elasticity of the deposited material as the crystallinity level of the filament material increases. Moreover, he

found that the inhomogeneous positioning of the crystalline areas in the mass of amorphous material generates an accentuated anisotropy of the mechanical characteristics. This anisotropy of the mechanical characteristics changes its spatial position as the deposition directions change. Vaes et al. [17] analyzed the ratio between the crystallinity of the filament polymer and that of the deposited material, finding that at high deposition rates the volume of amorphous material increases. It is predicted that a decrease in the cooling rate by using a hybrid heat source would decrease the volume of deposited amorphous material while maintaining the plasticity of the polymer. Savu et al. [18] studied the mode of polymer crystallization in 3D printing, both when using PLA and ABS, and when using polypropylene (PP). Moreover, together with Socol, he used hybrid sources for 3D printing, adding two other types of thermal sources to the traditional resistive source: a hot air jet or infrared radiation [19]. Savu also analyzed the melting of the polymer under conditions of heating in the microwave field [20]. Prajapati [21] reported improvements of the quality of the deposited material by using localized dispensing of hot air around the deposited filament. He reported that the enhanced thermal profile of the filament due to hot air dispensing results in an increased neck size, which translates to a 35% boost in thermal conductivity, a 19% improvement in tensile strength, and a 145% rise in tensile toughness. Unlike previous thermal techniques proposed for enhancing the FFF process, this method offers a highly localized, in situ thermal improvement of the immediate environment around the extruded filament and integrates effortlessly with the filament-dispensing nozzle. Cuiffo et al. [22] studied how the polymer structure changes in various 3D printing regimes. They concluded that there are changes in critical temperature ranges, but also changes in the resulting melting characteristics.

The proposed research addressed the preliminary study of the use of the laser beam as an additional heat source, in order to build a hybrid heating system. The purpose of such a hybrid system is to control the cooling rate of the deposited material. As seen above, a high cooling rate increases the proportion of

amorphous polymeric material at the expense of crystalline material. Such a situation produces a negative effect on the values of the plasticity characteristics of the deposited material.

The use of the laser beam for this purpose must be judiciously organized. The laser beam concentrates the energy on a relatively small surface, with the danger of thermal degradation of the material. At the same time, positioning on a relatively small surface can take the focal point off the material and introduce it into a material-free area of the FFF deposition. In such a case the laser beam will not produce any effect at the surface level, being only about energy consumption without producing anything. Positioning the beam over an area larger than a 0.2-0.6 mm radius disk, perhaps even at radius values above 5 mm, could provide thermal coverage on the deposition construct. But in order to establish the most suitable surface coating, it is necessary to study the thermal field produced by the resistive source together with the source which is the laser beam. Wasilewski et al. [23] investigated the thermal conditions during laser beam welding, which is similar to 3D printing in FFF process. He showed a significant shift in heat coupling, with conduction transitioning to deep penetration heating. Complementary work has been reported by Guo Ming et al. [24] who analysed the distribution of the temperature field in laser welding based on stainless steel. Mackwood [25] made a review of the literature regarding the reported research on thermal modelling and prediction of laser welding in metals. Other researchers [26-29] reported the use of 3D printing for printing natural materials.

2. MATERIALS AND EQUIPMENT

A PLA filament with a diameter of 1.75 mm and coming from commercial sources was used for the experiments. The printer used was from the Creality family, with minor configuration changes to attach a 1000 mW laser beam generating device. Figure 1 shows the setup for the 3D printing experiments. To protect the laser device, it has been designed a solid cooler to work in parallel with the other two standard coolers for electric devices.

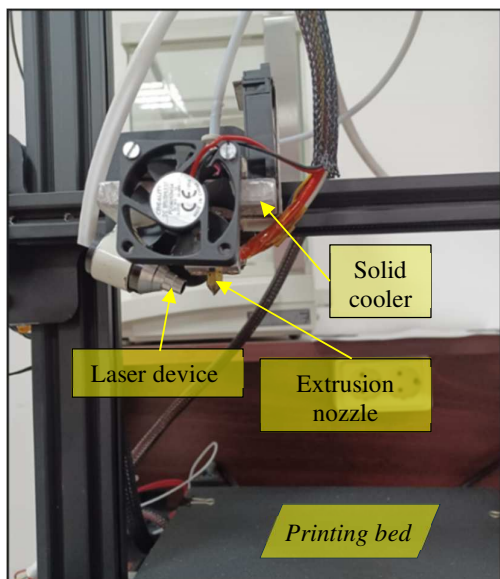


Fig. 1. 3D printing setup prepared for the experimental research

3. SIMULATION OF THERMAL FIELD

To be able to establish the correct and coherent parameters of the two heat sources it has been performed a simulation of the thermal field, to understand the evolution of the temperature values in time.

3.1 Simulation conditions

To simulate the thermal field during the printing through FFF process, ANSYS software has been used. It has been designed a specific piece, which is usually used to clamp electrical wires. The choice of this part to build by 3D printing was based on the fact that it has both sharp edges and rounded corners, but also relatively small holes (3 mm). The geometric and dimensional characteristics of the part to be printed are presented in Table 1.

Modelling parameters

Dimension	
Length	80 mm
Width	30 mm
Thickness	8 mm

Table 1

When designing the piece, the method of building by printing the pieces was taken into account, the structure being a scaffold type.

The geometric model was discretized in tetrahedral elements, the discretization parameters being presented in Table 2.

Table 2

Meshing elements			
Category	Value	Category	Value
Element size	0.48337 mm	Maximum Aspect Ratio	12.026
Tolerance	0.03127 mm	Percentage of elements with Aspect Ratio <3	87.9
Total nodes	182345		
Total elements	118654	Percentage of elements with Aspect Ratio >10	0.00943

For the thermal stress of the part under construction, a double thermal source was used, according to the sketch in figure 2. The two sources are the resistive source in the print setup and the second source was a surface heated by a laser beam. In order to have action on a larger surface, the laser was considered to be defocused at the surface level. The power transmitted by it will decrease, but its action will occur simultaneously on several deposited filament elements.

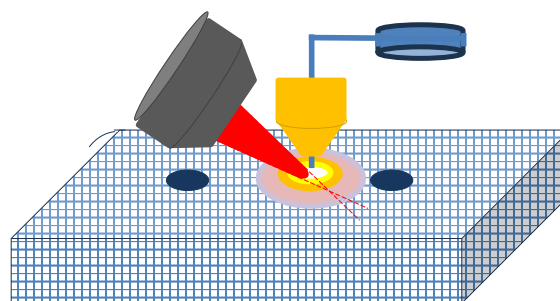


Fig. 2. Heat sources considered in the simulation

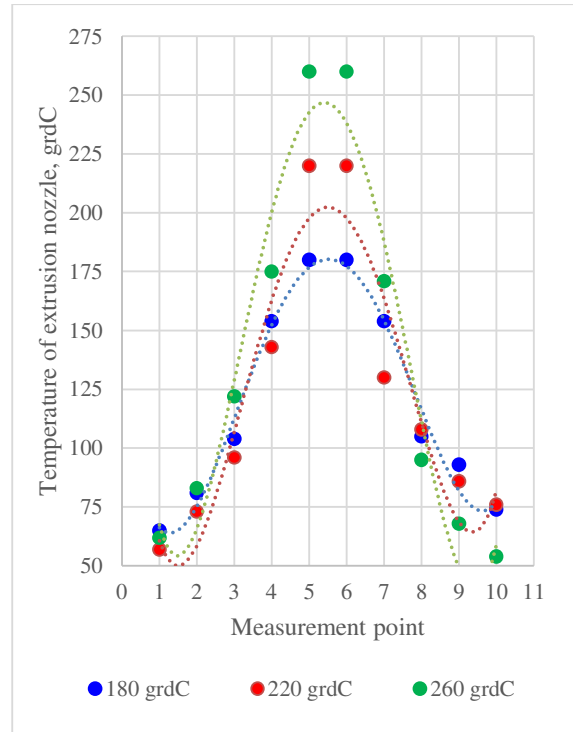
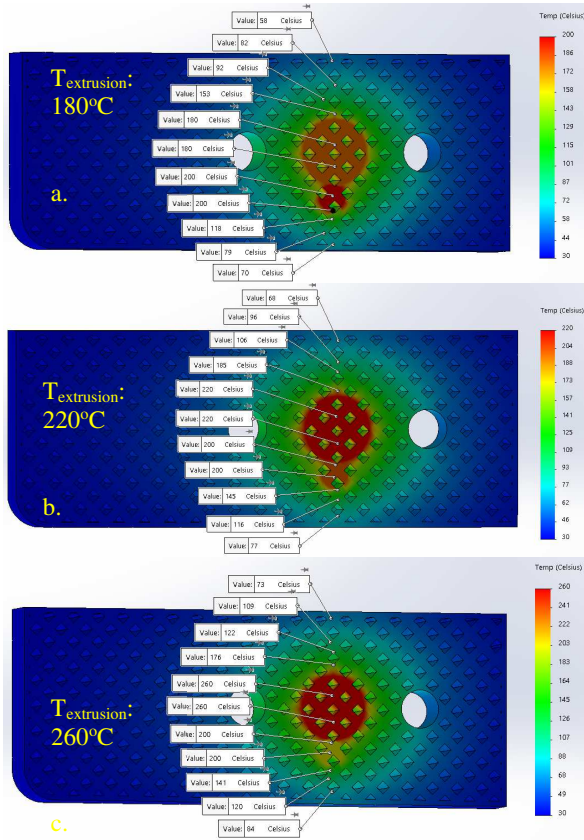
In the lower part of the part, heat sources were created over the entire surface, so as to simulate the print bed, normally heated to temperatures of 60-80°C. Cold points were equated to ambient temperature points.

Three distinct temperatures of the laser source were considered in the simulation: 180-220-260°C, these being covers for most polymers used in 3D printing. For each of the three temperatures, together with the resistive source (set at 200°C), the thermal fields at the surface layers of the deposition were simulated. The power of the laser source was changed to reach the desired temperatures to be maintained longer after the deposition pass.

The hybrid heating system was considered to be found in three distinct points: in an area that provides heat conduction in all directions; in a fringe area; and at the edge of one of the holes provided in the part.

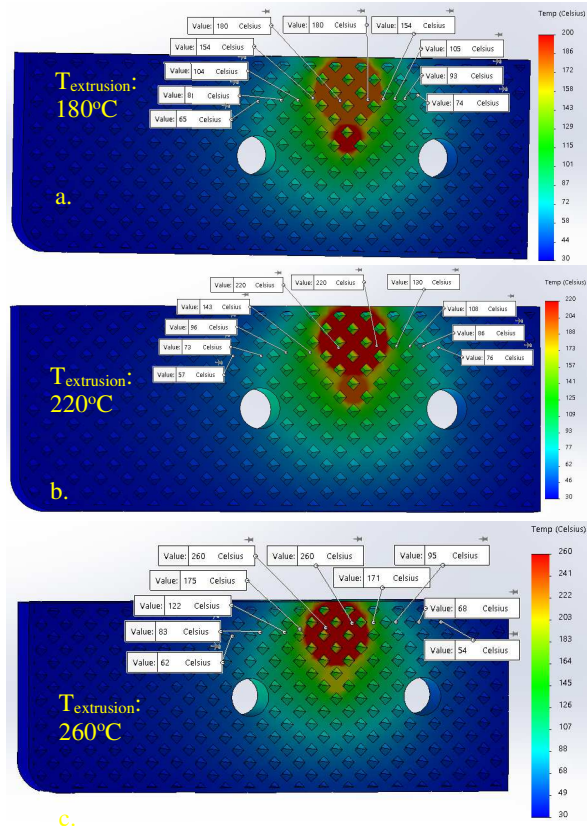
3.2 Results of simulation

Figures 3.a-c 4.a-c, and 5.a-c show the thermal maps resulted from the simulation process and Figures 3.d, 4.d and 5.d show the thermal field in all the three distinct points mentioned before.



d.

Fig. 3. a-c Thermal maps, d - Thermal field when the heat source spreads heat by conduction in all three directions



c.

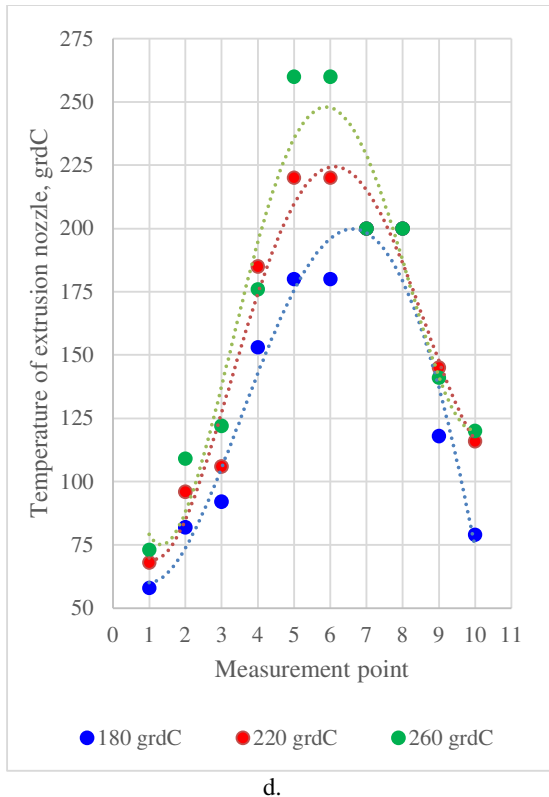


Fig. 4. a-c Thermal maps, d - Thermal field when build the margins

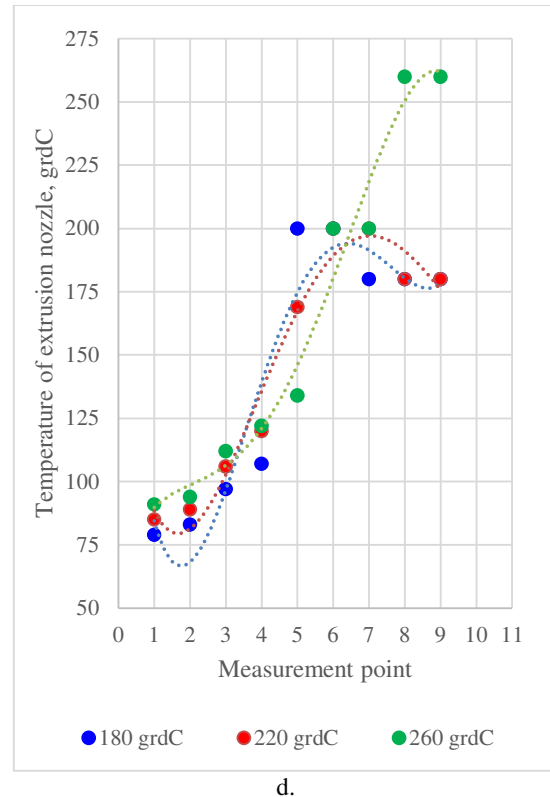
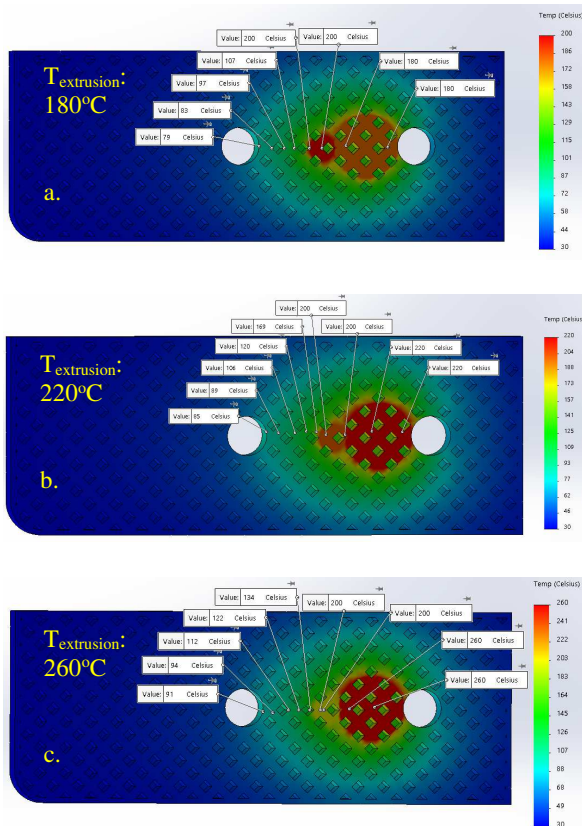


Fig. 5. a-c Thermal maps, d- Thermal field when build the margins of holes



3.3 Main conclusions on simulation results

Given the temperatures calculated by the simulation application, the ratio between the actions of the two sources changes: in certain situations, the resistive source is predominant and configures the thermal field, and in other situations the laser beam is the predominant one in the heating process, drawing the shape of the thermal field.

The temperature distribution is Gaussian where there is conduction in all three directions and partially Gaussian (open) in situations where part edges or hole edges are printed.

Faster temperature drops below 150°C are observed than drops from above 200°C to 150°C. This shows that the surface area of the sample must be kept above this value to prevent accelerated cooling.

4. EXPERIMENTAL PRINTING

The conclusions and the estimated values of the parameters of printing were tested through direct FFF printing, in the conditions concluded.

4.1 Printing parameters

The values of printing parameters, used in the experimental program, are presented in table 3.

Table 3

Printing parameters	
Parameter	Value
Extrusion nozzle temperature	220°C
Laser power	1000 mW
Surface covered in defocused mode	≈ 80 mm ²
Layer height	0.1 mm
Deposit angle	0°
Filling density	50%
Grid fill pattern	Grill
Raster angle	45°
Print speed	50 mm/s
Nozzle diameter	0.4 mm
Ambient temperature	23 °C

4.2 Thermal field during the printing process

During the printing process it has been recorded the thermal field using thermal camera of FLIR family (figure 6).

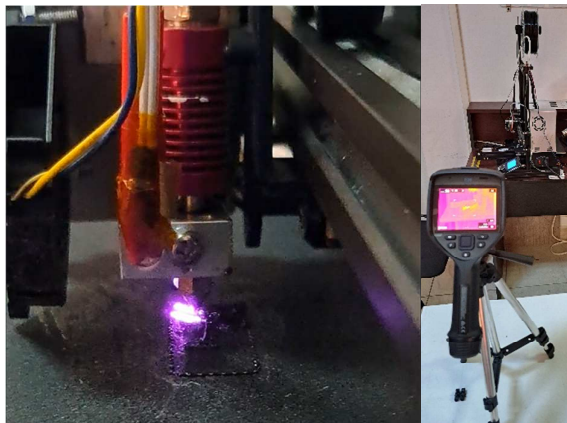
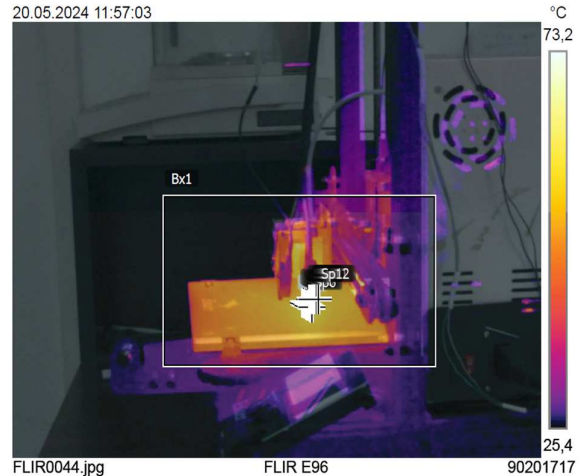


Fig. 6. Thermal field recorded during the printing process

The recorded values confirmed the models. The maximum deviation between the recorded values and calculated values was 17.6%, but it was recorded in areas of the thermal field with temperatures below 150°C.

Figure 7 shows example of recording.



Measurements

Point	Max	Temperature (°C)
Bx1		217,2 °C
Sp1		91,8 °C
Sp2		88,5 °C
Sp3		79,6 °C
Sp4		78,0 °C
Sp5		77,8 °C
Sp6		74,0 °C
Sp7		81,8 °C
Sp8		88,0 °C
Sp9		94,2 °C
Sp10		119,3 °C
Sp11		93,2 °C
Sp12		64,4 °C

Parameters

Emissivity	0.95
Refl. temp.	20 °C

Fig. 7. Recording of thermal field for a 220°C laser heating and 200°C heating produced by the resistive source

4.3 Analysis and main conclusions on the real thermal field

Heat flows predominantly through conduction, being able to use only the filament deposits during printing. There is, therefore, a resistance to the flow of heat, given by the voids of the scaffold structure.

The heat produced by the laser beam has the ability to transfer through three-dimensional conduction more easily than the heat produced by the resistive source. The laser beam has the ability to directly heat even layers below the surface.

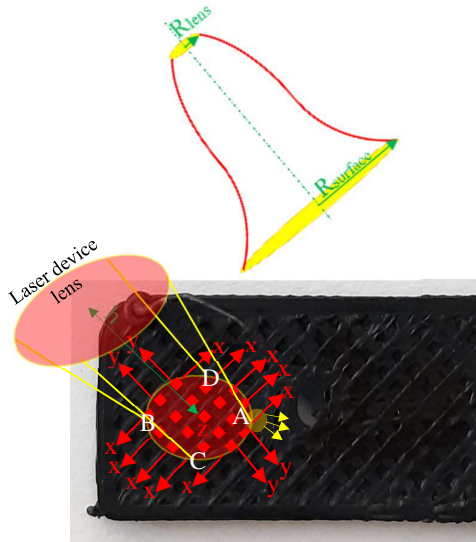


Fig. 8. Flowing of heat produced by the laser beam

According to this model, the heat flow can be estimated, taking account of the boundaries of the thermal field:

$$A: q_{vol}(x, y, z) = \frac{1}{1.2 \cdot h_{laser_cone}} \cdot \frac{q_0 \cdot n_{vol}}{\rho_{Gauss}^2 \cdot \pi} \cdot e^{-\left(\frac{x^2+y^2+z^2}{\rho_{Gauss}^2}\right)} \quad (1)$$

$$B: q_{vol}(x, y, z) = \frac{1}{0.8 \cdot h_{laser_cone}} \cdot \frac{q_0 \cdot n_{vol}}{\rho_{Gauss}^2 \cdot \pi} \cdot e^{-\left(\frac{x^2+y^2+z^2}{\rho_{Gauss}^2}\right)} \quad (2)$$

$$C, D: q_{vol}(x, y, z) = \frac{1}{h_{laser_cone}} \cdot \frac{q_0 \cdot n_{vol}}{\rho_{Gauss}^2 \cdot \pi} \cdot e^{-\left(\frac{x^2+y^2+z^2}{\rho_{Gauss}^2}\right)} \quad (3)$$

where:

h_{laser_cone} is the height of the laser cone (20 mm), q_0 is the heat flow through the lens ($\frac{1000 \text{ mW}}{\frac{\pi \cdot 8^2}{4}} = 19.90 \text{ mW/mm}^2$), n_{vol} is the laser power coefficient of efficiency (80-90%), ρ_{Gauss}^2 is the radius of the Gaussian volume of heat that acts on the surface (figure 8).

Given this resistance to heat flow, but also the acceleration of cooling when the temperature drops below 150°C, it is sufficient to intervene with the additional thermal source to ensure the maintenance of the deposition zone at temperatures higher than this value.

Future research could also reveal the minimum times required to maintain a temperature higher than 150°C.

5. VISUAL TESTING OF PRODUCTS

The printed pieces were analysed by visual testing (figures 9 a and b).



a.



b.

Fig. 9. Macroscopic image to evaluate the quality of the piece

3D printed samples with a hybrid heating source demonstrated a flattening of the deposited filament, the deposit changing its

shape from circular to ellipsoidal, almost rectangular.

The voids of the scaffold structure began to decrease in size. It is estimated that the material being more compact also contributes to an improvement of the mechanical characteristics. The material shows exaggerated heating in places, the scaffold structure being significantly less porous.

6. CONCLUSION

Using an additional heat source reconfigures the thermal field when printing with the FFF process.

The shape and dimensions of the thermal field depend on the ratio between the temperature produced by the additional source and that produced by the resistive source.

The laser beam can be considered as an additional heat source that can provide heating either pointwise or at the level of a surface.

To operate at the level of a surface, the focal point is positioned below the level of the part, so that the focal spot has the desired dimensions. Eventually, a defocus by moving the output lens can provide the desired surface for the beam action on the surface of the deposited part.

To create the geometric model, the scaffolding structure specific to 3D printed elements must be taken into account.

The temperature distribution is Gaussian, the situations in which the source acts at the edge of the part or at the edge of the holes it contains are different.

The distribution resulting from the simulation was confirmed by experiments, the model showing a maximum error of 17.6%, recorded at temperature values lower than 150°C.

Thermal transfer depends on the height of the laser beam cone, being inversely proportional to it.

Also inversely proportional is the relationship with the radius of the Gaussian shape of the laser beam.

In conclusion, it is possible to create a hybrid heating system that maintains the deposited material at a temperature higher than 150°C, reducing the cooling rate and preserving the values of the plasticity characteristics of the deposited polymer.

7. REFERENCES

- [1] Almaliki A., *The Processes and Technologies of 3D Printing*, International Journal of Advances in Computer Science and Technology, 4(10), pp. 161-165, 2015.
- [2] Kechagias J. D., Chaidas D., Vidakis N., Salonitis K., Vaxevanidis N.M., *Key parameters controlling surface quality and dimensional accuracy: a critical review of FFF process*, Materials and Manufacturing Processes, 37(9), pp. 963-984, 2022.
DOI: 10.1080 /10426914.2022.2032144
- [3] Manoj Prabhakar, M., et al., *A short review on 3D printing methods, process parameters and materials*, Materials Today: Proceedings, 45 pp.6108–6114, 2021.
- [4] J. Cui, J., Ren, L., et al., *3D Printing in the context of Cloud Manufacturing*, Robotics and Computer-Integrated Manufacturing, 74, p.102256, 2022.
- [5] Mallakpour, S., Tabesh, F., Mustansar, C., Hussain, *3D and 4D printing: From innovation to evolution*, Advances in Colloid and Interface Science, 294, p.102482, 2021.
- [6] Jandyal, A., Chaturvedi, I., Wazir, I., Raina, A., Irfan Ul Haq, M., *3D printing – A review of processes, materials and applications in industry 4.0*, Sustainable Operations and Computers, 3, pp.33–42, 2022.
- [7] <https://us.metoree.com/categories/3d-printer/#manufacturers>
- [8] <https://www.directindustry.com/industrial-manufacturer/fdm-3d-printer-110295.htm>
- [9] <https://www.raise3d.com/blog/what-is-fff-3d-printing/>
- [10] <https://www.3dsourced.com/rankings/best-fdm-3d-printer/>
- [11] Ligon, S. C., et al., *Polymers for 3D Printing and Customized Additive Manufacturing*, Chemical Reviews, 117 (15), pp.10212-10290, 2017.
- [12] Pritchard, E., *A Guide to 3D Printing Polymers and Materials*, <https://www.3devo.com/blog/guide-to-3d-printing-polymers-and-materials>
- [13] Arefin AME, Khatri NR, Kulkarni N, Egan PF., *Polymer 3D Printing Review: Materials, Process, and Design Strategies for Medical Applications*, Polymers, 13(9), p.1499, 2021.
<https://doi.org/10.3390/polym13091499>

- [14] Mohammed, A.A., Al Gawhari, F.J., *Types of Polymers Using in 3D Printing and Their Applications: A Brief Review*, European Journal of Theoretical and Applied Sciences, 1(16), pp.978-985, 2024.
DOI: 10.59324/ejtas.2023.1(6).94
- [15] Northcutt L.A., Orski S.V., Migler K.B., Kotula A.P., *Effect of processing conditions on crystallization kinetics during materials extrusion additive manufacturing*. Polymer, 154, pp.182–187, 2018.
- [16] Liao Y., Liu C., Coppola B., Barra G., Di Maio L., Incarnato L., Lafdi K., *Effect of Porosity and Crystallinity on 3D Printed PLA Properties*, Polymers, 11(9), p.1487, 2019.
DOI: 10.3390/polym11091487
- [17] Vaes D., Van Puyvelde P., *Semi-crystalline feedstock for filament-based 3D printing of polymers*. Progress in Polymer Science, 118, p.101411, 2021.
DOI:10.1016/j.progpolymsci.2021.101411
- [18] Ciornei M., Savu I. D., Sîrbu N. A., Savu S. V., Olei B. A., *Resistive-IR Hybrid Heating in FDM Printing*, Key Engineering Materials, 890, pp.157–164, 2021.
- [19] Savu I.D., Tarnita D., Savu S.V., Benga G.C, Cursaru L.M., Dragut D.V., Piticescu R.M., Tarnita D.N., *Composite Polymer for Hybrid Activity Protective Panel in Microwave Generation of Composite Polytetrafluoroethylene - Rapana Thomasiana*, Polymers, 13(15), p.2432, 2021
- [20] Savu I. D., Savu S. V., Benga G. C., *Thermal Runaway of the BaCO₃ + Fe₂O₃ homogenous mixture and mechanical alloys at the microwave heating*, Advanced Materials Research, 837, pp.185-189, 2013.
- [21] Prajapati, H., Salvi, S.S., Ravoori, D., Qasaimeh, M., Adnan, A., Jain, A., - *Improved print quality in fused filament fabrication through localized dispensing of hot air around the deposited filament*, Additive Manufacturing, 40, p. 101917, 2021.
<https://doi.org/10.1016/j.addma.2021.101917>
- [22] Cuiffo M.A., Snyder J., Elliott A.M., Romero N., Kannan S., Halada G.P., *Impact of the Fused Deposition (FDM) Printing Process on Polylactic Acid (PLA) Chemistry and Structure*, Appl. Sci. 7(6), p.579, 2017.
- [23] Wasilewski, E., et al., *Investigations on the thermal conditions during laser beam welding of high-strength steel 100Cr6*, Advances in Industrial and Manufacturing Engineering, 6, p.100118, 2023. ISSN 2666-9129,
<https://doi.org/10.1016/j.aime.2023.1001183>
- [24] Han G.M., Zhao, J., Li, J.Q., *Dynamic Simulation of the Temperature Field of Stainless-Steel Laser Welding*. Materials & Design, 28, pp.240-245, 2007.
DOI: 10.3390/app7060579
- [25] Mackwood, A. P.; Crafer, R. C., *Thermal modelling of laser welding and related processes: a literature review*. Optics and Laser Technology, 37(2), pp. 99-115, 2007.
DOI:10.1016/j.optlastec.2004.02.017
- [26] Savu, S.V., Tarnita, D., Benga, G.C., Dumitru, I., Stefan, I., Craciunoiu, N., Olei, A.B. and Savu, I.D., *Microwave technology using low energy concentrated beam for processing of solid waste materials from Rapana Thomasiana seashells*, Energies, 14(20), p.6780, 2021.
- [27] Tarnita, D., Berceanu, C. and Tarnita, C., *The three-dimensional printing—a modern technology used for biomedical prototypes*, Materiale plastice, 47(3), pp.328-334, 2010.
- [28] Cursaru, L.M., Iota, M., Piticescu, R.M., et al., *Hydroxyapatite from natural sources for medical applicatins*, Materials, 15(15), p.5091, 2022.
- [29] Tarnita, D., Tarnita, D.N., et al.,, 2009. *Modular adaptive bone plate for humerus bone osteosynthesis. Rom J Morphol Embryol*, 50(3), pp.447-452.

Sursa hibridă laser-rezistiv pentru procedeul de imprimare FFF

Unii autori au raportat utilizarea surselor hibride pentru încălzirea materialelor ce urmează a fi prelucrate prin diverse tehnologii de îmbinare sau sinterizare. Lucrarea prezintă rezultate ale unor cercetări exploratorii privind utilizarea unei surse de încălzire hibride, constând dintr-un cap de extrudare rezistiv și un fascicul laser defocalizat, pentru a încălzi materialul depus în imprimarea 3D prin procesul FFF. Această sursă hibridă urmărește reducerea vitezei de răcire a materialului depus pentru a îmbunătăți îmbinarea între două straturi succesive. De asemenea, s-a urmărit îmbunătățirea gradului de umplere printr-o apilatizare estimată a filamentului depus. A fost efectuată o simulare a acțiunii sursei hibride

de încălzire pentru a determina parametrii procesului. A fost realizat un model geometric solicitat termic similar cu situația reală. Câmpurile termice au fost simulate pentru diferite poziții ale sursei hibride pe suprafața piesei. Când au fost atinse temperaturile estimate pentru atingerea celor propuse, datele sistemului termic au fost preluate și transferate în sistemul fizic de imprimare 3D. Cu acești parametri s-au făcut depuneri, măsurându-se valorile temperaturii în diferite puncte ale câmpului termic de pe suprafața piesei. Măsurătorile au confirmat modelul geometric creat pentru simularea câmpului termic real. Probele realizate au fost analizate vizual și s-a ajuns la concluzia că depozitul nu mai are secțiune circulară, ci s-a aplatizat, ceea ce confirmă estimările inițiale: gradul de umplere a crescut cu 8-12%.

Remus SOCOL, PhD student, University of Craiova, Faculty of Mechanics, socol.remus.z2p@student.ucv.ro, +40352333431, 1, Calugareni, Drobeta-Tr.Severin, Romania.

Iulian ȘTEFAN, PhD student, University of Craiova, Faculty of Mechanics, iulian.stefan@edu.ucv.ro, +40352333431, 1, Calugareni, Drobeta-Tr.Severin, Romania.

Traian ȚUNESCU, PhD student, University of Craiova, Faculty of Mechanics, tunescu.traian.v7x@student.ucv.ro, +40352333431, 1, Calugareni, Drobeta-Tr.Severin, Romania.

Cristian CHIHAIA, PhD student, University of Craiova, Faculty of Mechanics, c.cristian.cde@gmail.com, +40 762 126 162, 107, Calea Bucuresti, Craiova, Romania.

Nicușor-Alin SÎRBU, PhD Eng., Senior Researcher, General Manager, NRD for Welding and Material Testing, asirbu@isim.ro, +40256491831, 30, Mihai Viteazu, Timișoara, Romania.

Ionel-Dănuț SAVU, PhD Professor, **corresponding author**, University of Craiova, Faculty of Mechanics, ionel.savu@edu.ucv.ro, +4035233343, 1, Calugareni, Drobeta-Tr.Severin, Romania.